



THE UNIVERSITY *of* EDINBURGH

Edinburgh Research Explorer

## Diabetes mellitus induces bone marrow microangiopathy

**Citation for published version:**

Oikawa, A, Siragusa, M, Quaini, F, Mangialardi, G, Katare, RG, Caporali, A, van Buul, JD, van Alphen, FPJ, Graiani, G, Spinetti, G, Kraenkel, N, Prezioso, L, Emanuelli, C & Madeddu, P 2010, 'Diabetes mellitus induces bone marrow microangiopathy' *Arteriosclerosis, thrombosis, and vascular biology*, vol. 30, no. 3, pp. 498-508. DOI: 10.1161/ATVBAHA.109.200154

**Digital Object Identifier (DOI):**

[10.1161/ATVBAHA.109.200154](https://doi.org/10.1161/ATVBAHA.109.200154)

**Link:**

[Link to publication record in Edinburgh Research Explorer](#)

**Document Version:**

Peer reviewed version

**Published In:**

*Arteriosclerosis, thrombosis, and vascular biology*

**Publisher Rights Statement:**

Copyright © 2010 by American Heart Association, Inc. All rights reserved

**General rights**

Copyright for the publications made accessible via the Edinburgh Research Explorer is retained by the author(s) and / or other copyright owners and it is a condition of accessing these publications that users recognise and abide by the legal requirements associated with these rights.

**Take down policy**

The University of Edinburgh has made every reasonable effort to ensure that Edinburgh Research Explorer content complies with UK legislation. If you believe that the public display of this file breaches copyright please contact [openaccess@ed.ac.uk](mailto:openaccess@ed.ac.uk) providing details, and we will remove access to the work immediately and investigate your claim.



Published in final edited form as:

Arterioscler Thromb Vasc Biol. 2010 March ; 30(3): 498–508. doi:10.1161/ATVBAHA.109.200154.

## Diabetes mellitus induces bone marrow microangiopathy

Atsuhiko Oikawa, PhD<sup>\*,1</sup>, Mauro Siragusa, MSc<sup>\*,1</sup>, Federico Quaini, MD<sup>2</sup>, Giuseppe Mangialardi, MD<sup>1</sup>, Rajesh G. Katare, MD<sup>1</sup>, Andrea Caporali, PhD<sup>1</sup>, Jaap D. van Buul, PhD<sup>3</sup>, Floris P.J. van Alphen, PhD<sup>3</sup>, Gallia Graiani, PhD<sup>2</sup>, Gaia Spinetti, PhD<sup>4</sup>, Nicolle Kraenkel, PhD<sup>1</sup>, Lucia Prezioso, BSc<sup>2</sup>, Costanza Emanuelli, PhD<sup>1</sup>, and Paolo Madeddu, MD<sup>1</sup>

<sup>1</sup>Experimental Cardiovascular Medicine, University of Bristol, UK <sup>2</sup>Department of Internal Medicine and Biomedical Science, University of Parma, Italy <sup>3</sup>Department of Molecular Cell Biology, University of Amsterdam, The Netherlands <sup>4</sup>IRCCS MultiMedica, Milan, Italy

### Abstract

**Objective**—The impact of diabetes on the bone marrow (BM) microenvironment was not adequately explored. We investigated whether diabetes induces microvascular remodeling with negative consequence for BM homeostasis.

**Methods and results**—We found profound structural alterations in BM from type-1 diabetic mice, with depletion of the hematopoietic component and fatty degeneration. Blood flow (fluorescent microspheres) and microvascular density (immunohistochemistry) were remarkably reduced. Flow cytometry verified the depletion of MECA-32<sup>POS</sup> endothelial cells (ECs). Cultured ECs from BM of diabetic mice showed higher levels of oxidative stress, increased activity of the senescence marker  $\beta$ -galactosidase, reduced migratory and network-formation capacities and increased permeability and adhesiveness to BM mononuclear cells. Flow cytometry analysis of lineage<sup>NEG</sup> c-Kit<sup>POS</sup> Sca-1<sup>POS</sup> (LSK) cell distribution along an *in vivo* Hoechst-33342 dye perfusion gradient documented that diabetes depletes LSK cells predominantly in the low-perfused part of the marrow. Cell depletion was associated to increased oxidative stress, DNA damage and activation of apoptosis. Boosting the anti-oxidative pentose phosphate pathway by benfotiamine supplementation prevented microangiopathy, hypoperfusion and LSK cell depletion.

**Conclusions**—We provide novel evidence for the presence of microangiopathy impinging on the integrity of diabetic BM. These discoveries offer the framework for mechanistic solutions of BM dysfunction in diabetes.

### Keywords

microangiopathy; diabetes; progenitor cells; oxidative stress

---

Diabetic patients suffer ischemic complications more frequently than non-diabetic subjects and also show a worse clinical outcome after an ischemic event. This prognostic disadvantage is partly dependent on diabetes-induced impairment of reparative angiogenesis. The contribution of circulating cells in maintenance of vascular integrity and recovery from ischemic complications has been also acknowledged. Tissue injury triggers the bone marrow (BM) to release progenitor cells (PCs) and monocytes with pro-angiogenic

---

**Corresponding author:** Prof. Paolo Madeddu, MD, Chair of Experimental Cardiovascular Medicine, University of Bristol, Bristol BS2 8HW, United Kingdom; Tel/fax 0044 (0)117 928 3904 [madeddu@yahoo.com](mailto:madeddu@yahoo.com).

\*Authors contributing equally to the study.

Disclosure: None

capacities into the peripheral circulation.<sup>1-3</sup> A default version of this cellular response may account for the weakened healing capacity in diabetes. However, whether diabetes may damage stem cells (SCs) inside the BM either directly or by altering their microenvironment remains to be elucidated.

Maintenance of BM homeostasis is dependent on the interaction between SCs and cells of the supportive microenvironment, where SCs self-renew, differentiate or die. Regulatory components of the niche include endothelial cells (ECs), mesenchymal cells and adipocytes. The cellular composition and location of the niche is associated with specialized functions. For instance, the vascular niche, composed of lineage-committed PCs, mature hematopoietic cells, stromal cells and cells of the fenestrated sinusoidal endothelium, preside over the trafficking of cells and solutes between the marrow and circulation.<sup>4</sup> The osteoblastic niche, located near the endosteal bone and its trabecular projections, is regarded as the main repository of primitive SCs of the marrow.<sup>5</sup> The low-oxygenated osteoblastic microenvironment is ideal to maintenance of SC quiescence, with SC differentiation occurring along the oxygen ascent toward the vasculature.<sup>6, 7</sup> However, some endosteal niches are well perfused, being enmeshed in microvessels that penetrate the bone, and are thereby equally influenced by signals from osteoblasts and ECs as well as by chemical cues from the circulation.<sup>8</sup> Furthermore, SCs scattered between the two main niches may represent transition entities moving back and forward between the endosteum and vasculature.<sup>9</sup>

In this study we investigated the status of vascular cells, hematopoietic cells and their niches in BM of diabetic mice. Results show profound marrow remodeling with depletion of the hematopoietic component and presence of a so-far-unreported form of microangiopathy. Importantly, cell depletion more prominently affected the osteoblastic niche, owing to the generation of a steeper perfusion gradient across the marrow. Inhibition of oxidative stress prevented BM microangiopathy, hypoperfusion and hematopoietic cell depletion.

## METHODS

A detailed, expanded Methods section is available in the online data supplement.

### Animal procedures

Experiments were performed in accordance with the *Guide for the Care and Use of Laboratory Animals* (the Institute of Laboratory Animal Resources, 1996) and with approval of the British Home Office. Type-1 diabetes (T1D) was induced in male CD1 mice (Charles River) by streptozotocin (STZ).<sup>10</sup> Age-matched male CD1 mice injected with the vehicle of STZ served as controls (C). Diabetes was assessed by measurement of glycemia at fast and glycosuria.

At 4 wk from diabetes induction, T1D subgroups were randomly assigned to receive benfotiamine (BFT, 70mg/kg body weight per d) or vehicle (1mmol/L HCl) in drinking water for 24 wk. Non-diabetic age-matched vehicle-treated male mice served as controls.

### Measurement of marrow blood flow (BF)

BF was assessed by fluorescent microspheres.

### Bone fixation, decalcification and sectioning

Bones were cleaned from muscle and connective tissue, fixed, decalcified and finally processed for paraffin-embedding.

## Morphometric measurements

Total volume of the marrow was computed from longitudinal and cross BM sections on an Olympus BX40 microscope. Giemsa, Trichrome Masson and Gomori staining was performed to identify the structural composition of BM.

## Immunostainings

To determine capillary and sinusoid density, BM sections were stained with Isolectin IB<sub>4</sub> (endothelial marker). Capillaries were recognized as small, regular endothelial structures, whose lumen-size does not exceed the diameter of an erythrocyte, while sinusoids were identified as irregular vessels, lined by a thin layer of Isolectin IB<sub>4</sub> positive ECs and able to contain several erythrocytes (Supplementary Fig. I). Arterioles were recognized by the vascular smooth muscle cell (VSMC) marker  $\alpha$ -smooth muscle actin ( $\alpha$ -SMA) and Isolectin IB<sub>4</sub>. The number of capillaries, sinusoids and arterioles was counted through the entire area of marrow and expressed as average density per mm<sup>2</sup> of tissue. Additionally, VE-cadherin-2 was used to visualize vascular niches. The endosteal surface lined by osteoblasts was visualized by an anti-N-cadherin antibody.<sup>11</sup> Mouse c-Kit and Sca-1 antigens were used to identify hematopoietic PCs and Ter119 to identify erythroid cells. DNA damage was assessed by staining for p-H2AX.<sup>12</sup> List of used antibodies is reported in Supplementary Table I.

## Selection of Bone Marrow Endothelial Cells (BMECs)

Freshly harvested BM cells were immunomagnetically depleted of CD11b-expressing cells to eliminate myeloid/monocyte fraction and cultured on 0.1% gelatin in DMEM 20% FBS, supplemented with AcSDKP in order to avoid SCs and fibroblasts contamination.<sup>13</sup> When confluent, cells were analysed by flow cytometry and immunocytochemistry to assess the expression of endothelium-specific markers. Using the same isolation protocol, confluent BMECs were used in functional studies.

## Functional and western blot assays on BMECs

Cell senescence was assessed by measuring  $\beta$ -Gal activity and reactive oxygen species (ROS) using MitoTracker® Red CM-H<sub>2</sub>XROS probe. Migration was assayed using a 24-well transwell setup and *in vitro* network formation on matrigel.<sup>14</sup> For static adhesion, BMECs were cultured to confluence on 0.1% gelatin-coated glass covers and treated overnight with Tumor Necrosis Factor- $\alpha$  (TNF- $\alpha$ , 10 ng/mL). Next, BM mononuclear cells (BMMNCs) from C mice were pre-labelled with Calcein-AM, resulting in green-fluorescence, and allowed to adhere for 30min on BMECs. Samples were then washed and adherent BMMNCs were counted using confocal fluorescent microscopy. To study the influence of flow, confluent BMECs were stimulated as above and mounted onto the microscope stage using a POC-mini chamber system (LaCon) and connected to a perfusion pump. Adhesion was visualized by phase-contrast microscopy and recorded in real-time. Trans-endothelial electrical resistance (TER) was evaluated by Electric Cell-substrate Impedance Sensing. To study trans-endothelial migration (TEM) of BMMNCs prepared from C or T1D mice; cells were pre-labeled with PKH67 (Sigma) and then left to migrate toward SDF-1 or vehicle through BMECs monolayers on coated transwell filters. Finally, protein expression of phosphorylated VE-cadherin and Pyk2 in BMECs was measured by western blot.

## Isolation of marrow cells from trabecular bone

Hematopoietic Stem Cell Isolation Kit (Millipore UK) was used for isolation of marrow cells from trabecular bone.

### Colony forming cell (c.f.c) assay

Freshly harvested BM cells from trabecular bone were seeded on methycellulose ( $1 \times 10^4$  cells/dish) and cultured for 14d before scoring colonies.

### Flow cytometry analysis

Freshly harvested BM cells were washed with ice-cold Hank's balanced salt solution containing 0.5% bovine serum albumin and 0.02% sodium azide. BM cells were then stained in the same buffer with anti Lineage Mixture (Alexa 488), anti-Sca-1 (PE), anti-CD34 (Alexa 647) and anti-c-Kit (Alexa 750 or Alexa 647 when CD34 was omitted). To recognize ECs, BM cells were stained with anti-MECA-32 (Biotin) followed by Streptavidin-APC conjugate. To detect apoptosis, BM cells were stained with Annexin V (FITC). ROS positive cells were identified using CM-H<sub>2</sub>DCFDA. Distribution of BM cells according to BM perfusion gradient was evaluated using the Hoechst 33342 (Hoe) dye.<sup>7</sup> Briefly, Hoe was injected through the tail vein and the animals sacrificed 10min later to collect the hindlimb BM. Cells in microenvironments that are well perfused by blood are those exposed to the highest concentrations of Hoe, whereas cells in microenvironments that are less perfused are exposed to lower concentrations of Hoe. Flow cytometry identification of cells stained high or low with Hoe (Hoe<sup>high</sup> and Hoe<sup>low</sup>, respectively) allowed for recognition of cell distribution in high-perfused vs. low-perfused regions of BM (Supplementary Fig. II). Flow cytometry was performed on FACSCanto II and FACSLSR11 (BD Biosciences) equipped with FACSDiva software (BD Biosciences). Data were represented using "Logical" displays. List of used antibodies is reported in Supplementary Table II.

### Statistics

Differences between multiple groups were compared by analysis of variance (ANOVA) followed by a Holm-Sidak multiple comparison test. Two-group analysis was performed by t-test (paired or unpaired as appropriate). Probability-values of less than 0.05 were considered significant.

## RESULTS

### Diabetes reduces BM volume and cellularity

First, we compared the BM structure of T1D mice at 27-30 wk from the onset of diabetes to age-matched non-diabetic controls. Diabetes remarkably reduced the hematopoietic fraction and caused fat accumulation and osteopenia (Fig. 1). No structural alteration was observed at 10d after diabetes induction (data not shown), discounting an acute toxic effect of STZ on the BM.

### Microangiopathy in diabetic BM

Cumulative vascular density was reduced by 2.9-fold in BM of T1D mice ( $P < 0.001$  vs. C). Analysis of perfused vessels, identified by binding of intracardially-injected isolectin IB<sub>4</sub>, revealed a consistent reduction of sinusoids, capillaries and arterioles. Furthermore, the microvasculature appeared fragmented with bleeding into the surrounding marrow (Fig. 2a-d).

Flow cytometry analysis of BM-single cell suspensions, using an antibody specific for the EC marker MECA-32, confirmed BMEC depletion and increased BMEC apoptosis in diabetes (Fig. 2e,f).

## Functional alterations of diabetic BMECs

BMECs were isolated from T1D and C mice and their purity was confirmed by flow cytometry and immunocytochemistry (Supplementary Fig. III). We found that T1D BMECs express higher levels of mitochondrial ROS (Fig. 3a) and cell senescence marker  $\beta$ -galactosidase (Fig. 3b), are unresponsive to chemo-attractant stimuli, like SDF-1 and VEGF-A (Fig. 3c), and fail to form network structures on matrigel (Fig. d). Furthermore, we observed an increased adhesion of BMMNCs to T1D BMECs under static conditions and after introduction of shear flow (Fig. 3e,f).

Another hallmark of diabetic microvasculature is its augmented permeability. Confluent T1D BMECs showed a  $14\pm 2\%$  reduction in trans-endothelial resistance compared to C BMECs ( $P<0.05$ ), which was abrogated by the ROS scavenger N-Acetyl-cysteine (N-Ac), pinpointing oxidative stress as a determinant of altered cell-cell interaction. ROS facilitates trans-endothelial migration of BM-derived PCs through phosphorylation of VE-cadherin by the redox-sensitive protein tyrosine kinase 2 (Pyk2).<sup>15, 16</sup> We found that T1D BMECs have higher phosphorylation levels of VE-cadherin (at tyrosine 731, the  $\beta$ -catenin binding site) and Pyk2 (at tyrosine 402, which is the auto-phosphorylation site for Pyk2) compared with C BMECs (Fig. 3g). Furthermore, T1D BMMNCs transmigrate as efficiently as C BMMNCs in the presence of non-diabetic endothelium (Fig. 3h, left). In contrast, non-specific migration of BMMNCs was enhanced and SDF-1-stimulated migration was abolished in the presence of diabetic endothelium, thus suggesting endothelial barrier dysfunction in T1D (Fig. 3h, right).

## Diabetes causes depletion of BM Sca-1<sup>POS</sup>c-Kit<sup>POS</sup> cells

Immunohistochemical analysis documented the reduction of Sca-1<sup>POS</sup>c-Kit<sup>POS</sup> (SK) cells in BM of T1D, especially at the level of the osteoblastic niche, identified by staining osteoblast lining with N-cadherin (Fig. 4 and Supplementary Fig. IV). Furthermore, considering longitudinal and coronal sections of BM, we verified that the distance of SK cell clusters of the osteoblastic niche to sinusoids is longer in marrow of T1D mice ( $9.0\pm 0.4$  cell diameters) compared to C ( $5.5\pm 0.4$  cell diameters,  $P<0.001$ ).

Flow cytometry analysis confirmed the effect of diabetes on reducing the relative frequency of Lineage<sup>neg</sup> SK (LSK) cells in marrow of the femoral cavity or trabecular bone, a porous plexus enriched of SCs and osteoblasts (Fig. 5a).<sup>5</sup> We also found that the sub-fraction of primitive CD34<sup>neg</sup>LSK cells is remarkably reduced in T1D marrow ( $3.6\pm 0.7$  per 100,000 BM cells) compared to C ( $27.0\pm 3.0$  per 100,000 BM cells,  $P<0.01$ ). Concordantly, colony forming unit assays showed a reduced formation of multipotent PC colonies (c.f.u. GEMM) by trabecular BM cells of T1D mice (Fig. 5b). However, the colony forming activity of lineage-committed PCs was similar in diabetic and control mice, suggesting compensation downstream to multipotent PCs.

## Diabetes reduces BM perfusion

T1D mice showed a remarkably reduced BM perfusion at the level of femur ( $0.17\pm 0.01$  vs.  $0.27\pm 0.02$  mL/min/gm in C,  $P<0.01$ ) and tibia ( $0.11\pm 0.01$  vs.  $0.18\pm 0.03$  mL/min/gm in C,  $P<0.01$ ).

## Predominant LSK cell depletion in the hypoperfused part of the marrow

We then determined the relative position of LSK cells with respect to *in vivo* Hoe dye perfusion gradient.<sup>7</sup> Hoe was injected intravenously and then the degree of uptake of the dye by BM cells from different locations was evaluated by flow cytometry. We found that 53% of total LSK cells are located in the Hoe<sup>low</sup> perfusion region of C BM, but this fraction decreased to 21% in T1D BM (Fig. 6a, central panel). Reversing the gating procedure, we

analyzed the abundance of LSK cells in total cells and lympho-monocyte (LM) fraction of each Hoe perfusion area (Fig. 6b). Results confirmed the selective depletion of LSK cells of the low-perfused zone of T1D BM, whereas the high-perfused zone, which corresponds to the predominant localization of MECA-32<sup>POS</sup> BMECs (e.g. the vascular niche) was relatively preserved. MECA32<sup>POS</sup> ECs were overall reduced in T1D BM (Fig. 6c) and, considering their relative distribution, also shifted from the low to the high Hoe perfusion area (Fig. 6a, right panel).

### Increased oxidative stress in diabetic BM

Next, we measured levels of oxidative stress in BM cells using CM-H<sub>2</sub>DCFDA, a cell-permeable intracellular ROS indicator. Flow cytometry analysis showed that ROS<sup>high</sup> SK cells are greatly increased in T1D BM (Fig. 7a). We also verified the presence of higher mitochondrial ROS levels in BMMNCs from T1D trabecular marrow, using MitoTracker Red CM-H<sub>2</sub>XROS (Fig. 7b).

Excessive oxidative stress reportedly causes DNA damage and reduces the lifespan of BMSCs.<sup>17</sup> Levels of p-H2AX (Ser139), a marker of double DNA strand breaks, were 2.5-fold higher in T1D BM cells compared to C (Fig. 7c). Since H2AX is phosphorylated by ATM, we analyzed ATM expression by qPCR and found it 2.6-fold higher in T1D BM cells compared to C. Furthermore, flow cytometry analysis of Annexin V-positive cells unravelled the increased apoptosis of SK cells from BM of T1D mice (Fig. 7d).

### Stimulation of anti-oxidative mechanism prevents microangiopathy and LSK cell depletion

We found that diabetes reduces the activity of transketolase and G6PDH, the rate-limiting enzymes of the pentose phosphate pathway, which represents a fundamental source of anti-oxidant equivalents and substrates for DNA synthesis and repair (Fig. 8a,b).

We then asked whether activation of the above anti-oxidative mechanism may protect BM from diabetes-induced damage. Boosting the thiamine-dependent enzyme transketolase by BFT supplementation (Fig. 8a) restored G6PDH activity (Fig. 8b) and prevented microangiopathy (Fig. 8c) and hypo-perfusion of diabetic BM (Fig. 8d). Furthermore, BFT prevented oxidative stress (Fig. 8e) and p-H2AX elevation (Fig. 8f) in T1D BM cells. Importantly, these effects of BFT were associated to prevention of LSK cell depletion, both in terms of absolute number (Fig. 8g) and relative proportion to total BM cells (Fig. 8h), and inhibition of apoptosis (Fig. 8i). Analysis of cell distribution across the Hoe perfusion gradient confirmed BFT's protective action against diabetes-induced LSK cell depletion (Fig. 8jk).

## DISCUSSION

Here we show for the first time the presence of diabetic microangiopathy altering the marrow milieu. Microvascular rarefaction was associated with endothelial dysfunction, encompassing reduced migratory capacity, impaired angiogenic activity, increased adhesiveness and endothelial barrier disruption. Importantly, these defects were observed after culturing diabetic bone marrow endothelial cells in normal glucose, in line with the recent demonstration of epigenetic changes caused by transient hyperglycemia.<sup>18</sup>

Previous studies have documented the important role of the bone marrow endothelium in maintenance of marrow homeostasis through paracrine and physical interaction with other cells of the marrow.<sup>19, 20</sup> Another important function of BM vasculature is to deliver nutrients and oxygen to marrow cells. The peculiar distribution of microvasculature creates differentially perfused environments across the marrow. The most primitive stem cells are believed to reside in the osteoblastic niche at the lowest end of the physiologic perfusion

gradient, protected from oxidative stress.<sup>6, 7</sup> However, recent studies demonstrated that a large fraction of endosteal stem cells is enmeshed in vessel networks.<sup>21</sup> In diabetic BM, the ongoing microvascular rarefaction inevitably alters the path-length for oxygen and nutrient diffusion and, as a consequence, an increasing fraction of marrow becomes critically hypoperfused and secluded from the influence of the vascular niche. Our results indicate that LSK cells of the osteoblastic niche can barely survive in such a harsh environment. However, the bone marrow vasculature can offer an ultimate shelter, as documented by the relative conservation of LSK cells in the peri-vascular space. To the best of our knowledge, the only precedent for marrow cell depletion in the hypoxic microenvironment, often identified with the osteoblastic niche, is represented by the hematopoietic decline described in aging rodents.<sup>6</sup> The model of accelerated senescence fits very well with diabetic BM remodeling, since in both conditions fat accumulation occurs along with osteopenia. The mechanism which underpins aging- and diabetes-induced increases in adipocyte abundance remains unknown. Fat accumulation could serve not only to fill the empty marrow, pushing marrow cells toward the vasculature, but also participate in the ongoing diabetic remodeling by secreting paracrine factors and pro-inflammatory cytokines.<sup>22</sup> Of note, a similar remodeling was observed in obese leptin-receptor mutant mice, a model of insulin-resistant type-2 diabetes (P. Madeddu, unpublished observations, 2009).

The physiological gradient of ROS acts as a signaling mechanism governing functional compartmentalization of stem cells. Those precious cells, necessary for regeneration of almost all the rest of the whole organism, reside in the “low risk zone” ideal for maintenance of quiescence. The function of the ROS<sup>high</sup> zone adjacent to the marrow vasculature is instead to facilitate stem cell maturation.<sup>6</sup> Under pathologic conditions, however, excessive production of ROS might endanger the viability of stem cells. Genetically modified mice, lacking essential components of the regulatory system that maintain ROS within the physiologic range, show accelerated stem cell senescence and progressive bone marrow failure,<sup>23-25</sup> replicating the situation observed in mice exposed to the oxidant buthionine sulfoxime.<sup>17</sup> Our data show that an elevation in intra-cellular ROS infringes on DNA integrity and compromises marrow cell function in a model of common human disease. Different mechanisms might contribute to increase oxidative stress in LSK cells, including critical hypoperfusion and high glucose, which are both potent activators of ROS generation by mitochondrial complex III,<sup>26, 27</sup> as well as exposure to ROS from other cellular sources. For instance, transition metal iron from extravasated erythrocytes can be a potent source of ROS *via* the Fenton reaction. Another mechanism consists of the reduced activity of anti-oxidative mechanisms, such as the pentose phosphate pathway. In line with the latter, benfotiamine buffered the diabetes-induced disruptive effect on LSK cells.

The extensive remodeling of bone marrow observed in diabetic mice may not inspire therapeutic optimism. However, previous studies showed that glucose-lowering therapies can restore progenitor cell function to some extent.<sup>reviewed in 28</sup> Similarly, in genetically-modified animals unable to modulate ROS production, anti-oxidant administration restored the reconstitutive capacity of hematopoietic stem cells, thereby preventing bone marrow failure.<sup>23, 24</sup> Our study newly shows that benfotiamine stimulates anti-oxidative defense through activation of transketolase and protects vascular and LSK cells from oxidative stress and apoptosis.

In conclusion, our results demonstrate the deleterious effect of diabetes on bone marrow homeostasis. Our characterization of the molecular and cellular signature of diabetic pathology in bone marrow along with successful results of benfotiamine treatment may lead to beneficial therapies for human disease. Whether thiamine-derivatives may clinically reverse BM failure in diabetes represents the objective of future investigation.



### CONDENSED ABSTRACT

We newly demonstrate the presence of microangiopathy in BM of diabetic mice, associated with LSK cells depletion according to a steeper perfusion gradient from the vascular to osteoblastic niche. We show that diabetic microangiopathy can be prevented together with LSK depletion by improving anti-oxidative defense mechanism.

### Supplementary Material

Refer to Web version on PubMed Central for supplementary material.

### Acknowledgments

*Funding:* Wellcome Trust (083018/Z/07/Z), BHF (PG/06/096/21325, FS/06/083/21828), EC-FP7-53861 to P.M.; the Dutch Heart Foundation (2005T039) and NWO Veni grant (916.76.053) to J.D.vB. and F.P.J.vA; BIOSCENT FP7-NMP-214539, MIUR Grant (AL2YNC) and THEAPPL to F.Q.; C.E. holds a BHF Basic Science fellowship (BS/05/01).

### REFERENCES

- Asahara T, Kawamoto A. Endothelial progenitor cells for postnatal vasculogenesis. *Am J Physiol Cell Physiol.* 2004; 287:C572–579. [PubMed: 15308462]
- Dimmeler S. ATVB in focus: novel mediators and mechanisms in angiogenesis and vasculogenesis. *Arterioscler Thromb Vasc Biol.* 2005; 25:2245. [PubMed: 16258151]
- Fischer C, Schneider M, Carmeliet P. Principles and therapeutic implications of angiogenesis, vasculogenesis and arteriogenesis. *Handb Exp Pharmacol.* 2006:157–212. [PubMed: 16999228]
- Jin DK, Shido K, Kopp HG, Petit I, Shmelkov SV, Young LM, Hooper AT, Amano H, Avecilla ST, Heissig B, Hattori K, Zhang F, Hicklin DJ, Wu Y, Zhu Z, Dunn A, Salari H, Werb Z, Hackett NR, Crystal RG, Lyden D, Rafii S. Cytokine-mediated deployment of SDF-1 induces revascularization through recruitment of CXCR4+ hemangiocytes. *Nat Med.* 2006; 12:557–567. [PubMed: 16648859]
- Calvi LM, Adams GB, Weibrecht KW, Weber JM, Olson DP, Knight MC, Martin RP, Schipani E, Divieti P, Bringhurst FR, Milner LA, Kronenberg HM, Scadden DT. Osteoblastic cells regulate the haematopoietic stem cell niche. *Nature.* 2003; 425:841–846. [PubMed: 14574413]
- Jang YY, Sharkis SJ. A low level of reactive oxygen species selects for primitive hematopoietic stem cells that may reside in the low-oxygenic niche. *Blood.* 2007; 110:3056–3063. [PubMed: 17595331]
- Parmar K, Mauch P, Vergilio JA, Sackstein R, Down JD. Distribution of hematopoietic stem cells in the bone marrow according to regional hypoxia. *Proc Natl Acad Sci U S A.* 2007; 104:5431–5436. [PubMed: 17374716]
- Lo Celso C, Fleming HE, Wu JW, Zhao CX, Miake-Lye S, Fujisaki J, Cote D, Rowe DW, Lin CP, Scadden DT. Live-animal tracking of individual haematopoietic stem/progenitor cells in their niche. *Nature.* 2009; 457:92–96. [PubMed: 19052546]
- Kiel MJ, Morrison SJ. Uncertainty in the niches that maintain haematopoietic stem cells. *Nat Rev Immunol.* 2008; 8:290–301. [PubMed: 18323850]
- Gadau S, Emanuelli C, Van Linthout S, Graiani G, Todaro M, Meloni M, Campesi I, Invernici G, Spillmann F, Ward K, Madeddu P. Benfotiamine accelerates the healing of ischaemic diabetic limbs in mice through protein kinase B/Akt-mediated potentiation of angiogenesis and inhibition of apoptosis. *Diabetologia.* 2006; 49:405–420. [PubMed: 16416271]
- Zhang J, Niu C, Ye L, Huang H, He X, Tong WG, Ross J, Haug J, Johnson T, Feng JQ, Harris S, Wiedemann LM, Mishina Y, Li L. Identification of the haematopoietic stem cell niche and control of the niche size. *Nature.* 2003; 425:836–841. [PubMed: 14574412]
- Li XM, Hu Z, Jorgenson ML, Wingard JR, Slayton WB. Bone marrow sinusoidal endothelial cells undergo nonapoptotic cell death and are replaced by proliferating sinusoidal cells in situ

- maintain the vascular niche following lethal irradiation. *Exp Hematol.* 2008; 36:1143–1156. [PubMed: 18718416]
13. Wang QR, Wang BH, Huang YH, Dai G, Li WM, Yan Q. Purification and growth of endothelial progenitor cells from murine bone marrow mononuclear cells. *J Cell Biochem.* 2008; 103:21–29. [PubMed: 17471503]
  14. Krankel N, Katare RG, Siragusa M, Barcelos LS, Campagnolo P, Mangialardi G, Fortunato O, Spinetti G, Tran N, Zacharowski K, Wojakowski W, Mroz I, Herman A, Fox JE, Manning, MacDonald PE, Schanstra JP, Bascands JL, Ascione R, Angelini G, Emanuelli C, Madeddu P. Role of kinin B2 receptor signaling in the recruitment of circulating progenitor cells with neovascularization potential. *Circ Res.* 2008; 103:1335–1343. [PubMed: 18927465]
  15. van Buul JD, Voermans C, van den Berg V, Anthony EC, Mul FP, van Wetering S, van der Schoot CE, Hordijk PL. Migration of human hematopoietic progenitor cells across bone marrow endothelium is regulated by vascular endothelial cadherin. *J Immunol.* 2002; 168:588–596. [PubMed: 11777950]
  16. Allingham MJ, van Buul JD, Burrige K. ICAM-1-mediated, Src- and Pyk2-dependent vascular endothelial cadherin tyrosine phosphorylation is required for leukocyte transendothelial migration. *J Immunol.* 2007; 179:4053–4064. [PubMed: 17785844]
  17. Ito K, Hirao A, Arai F, Takubo K, Matsuoka S, Miyamoto M, Ohmura M, Naka K, Hosokawa K, Ikeda Y, Suda T. Reactive oxygen species act through p38 MAPK to limit the lifespan of hematopoietic stem cells. *Nat Med.* 2006; 12:446–451. [PubMed: 16565722]
  18. El-Osta A, Brasacchio D, Yao D, Pocai A, Jones PL, Roeder RG, Cooper ME, Brownlee M. Transient high glucose causes persistent epigenetic changes and altered gene expression during subsequent normoglycemia. *J Exp Med.* 2008; 205:2409–2417. [PubMed: 18809715]
  19. Avecilla ST, Hattori K, Heissig B, Tejada R, Liao F, Shido K, Jin DK, Dias S, Zhang F, Hartman TE, Hackett NR, Crystal RG, Witte L, Hicklin DJ, Bohlen P, Eaton D, Lyden D, de Sauvage F, Rafii S. Chemokine-mediated interaction of hematopoietic progenitors with the bone marrow vascular niche is required for thrombopoiesis. *Nat Med.* 2004; 10:64–71. [PubMed: 14702636]
  20. Levesque JP, Henty J, Takamatsu Y, Simmons PJ, Bendall LJ. Disruption of the CXCR4/CXCL12 chemotactic interaction during hematopoietic stem cell mobilization induced by GCSF or cyclophosphamide. *J Clin Invest.* 2003; 111:187–196. [PubMed: 12531874]
  21. Kiel MJ, Yilmaz OH, Iwashita T, Yilmaz OH, Terhorst C, Morrison SJ. SLAM family receptors distinguish hematopoietic stem and progenitor cells and reveal endothelial niches for stem cells. *Cell.* 2005; 121:1109–1121. [PubMed: 15989959]
  22. Naveiras O, Nardi V, Wenzel PL, Hauschka PV, Fahey F, Daley GQ. Bone-marrow adipocytes as negative regulators of the haematopoietic microenvironment. *Nature.* 2009; 460:259–263. [PubMed: 19516257]
  23. Tothova Z, Kollipara R, Huntly BJ, Lee BH, Castrillon DH, Cullen DE, McDowell EP, Lazo-Kallanian S, Williams IR, Sears C, Armstrong SA, Passegue E, DePinho RA, Gilliland DG. FoxOs are critical mediators of hematopoietic stem cell resistance to physiologic oxidative stress. *Cell.* 2007; 128:325–339. [PubMed: 17254970]
  24. Ito K, Hirao A, Arai F, Matsuoka S, Takubo K, Hamaguchi I, Nomiyama K, Hosokawa K, Sakurada K, Nakagata N, Ikeda Y, Mak TW, Suda T. Regulation of oxidative stress by ATM is required for self-renewal of haematopoietic stem cells. *Nature.* 2004; 431:997–1002. [PubMed: 15496926]
  25. Chen C, Liu Y, Liu R, Ikenoue T, Guan KL, Liu Y, Zheng P. TSC-mTOR maintains quiescence and function of hematopoietic stem cells by repressing mitochondrial biogenesis and reactive oxygen species. *J Exp Med.* 2008; 205:2397–2408. [PubMed: 18809716]
  26. Du X, Matsumura T, Edelstein D, Rossetti L, Zsengeller Z, Szabo C, Brownlee M. Inhibition of GAPDH activity by poly(ADP-ribose) polymerase activates three major pathways of hyperglycemic damage in endothelial cells. *J Clin Invest.* 2003; 112:1049–1057. [PubMed: 14523042]
  27. Klimova T, Chandel NS. Mitochondrial complex III regulates hypoxic activation of HIF. *Cell Death Differ.* 2008; 15:660–666. [PubMed: 18219320]

28. Fadini GP. An underlying principle for the study of circulating progenitor cells in diabetes and its complications. *Diabetologia*. 2008; 51:1091–1094. [PubMed: 18478199]

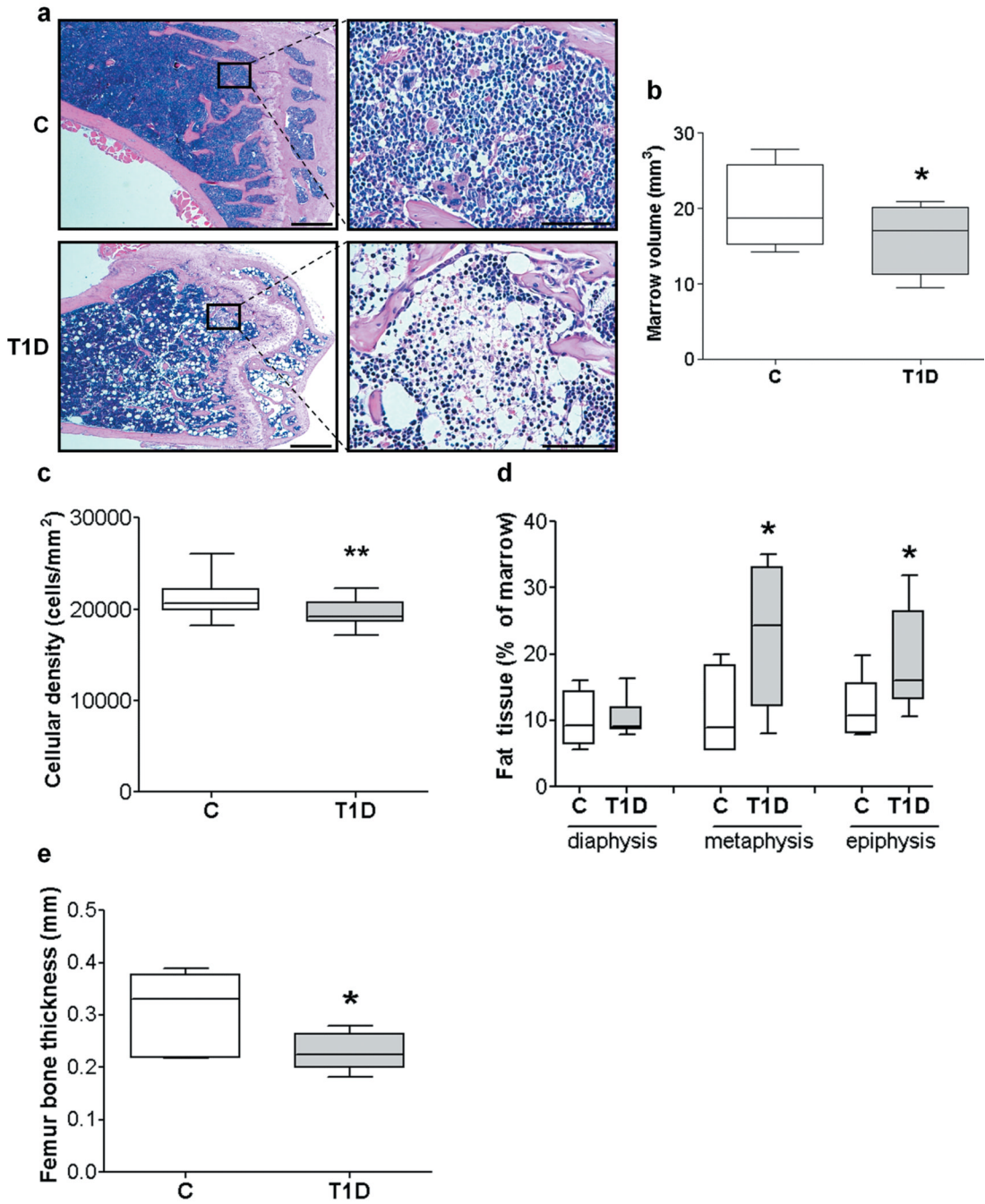


**Figure 1. BM remodelling in T1D mice**

(a) Representative images of H&E staining of femurs from C and T1D mice (scale bars: 500  $\mu$ m). High magnifications of epiphysis and metaphysis show decreased cell density and empty spaces corresponding to fat accumulation in the marrow of the T1D mouse (scale bars: 100  $\mu$ m). Box and whiskers graphs show min to max values of marrow volume (b), marrow cellular density (c), relative abundance of fat (d) and bone thickness (e). n=7 mice per group. \* $P$ <0.05 and \*\* $P$ <0.01 vs. C.

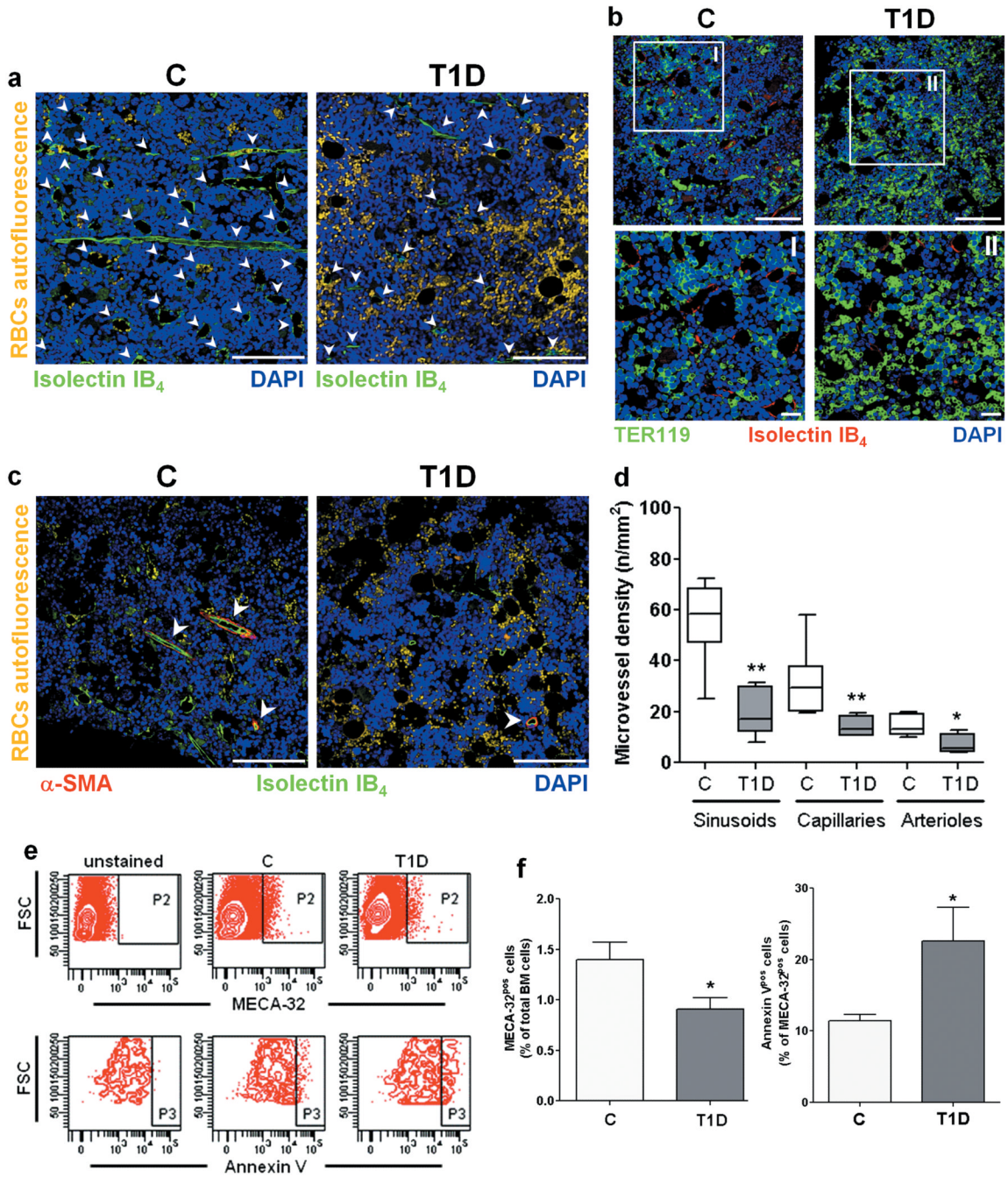


**Figure 2. Microangiopathy in BM of T1D mice**

Reduced vascular density and erythrocyte extravasation in T1D BM (a-d). Arrowheads point vascular structures. Scale bars: 100 $\mu$ m and 20 $\mu$ m (I and II). BMEC depletion and increased BMEC apoptosis in diabetes (e,f). n=8 mice per group. \*P<0.05, \*\*P<0.01 vs. C.

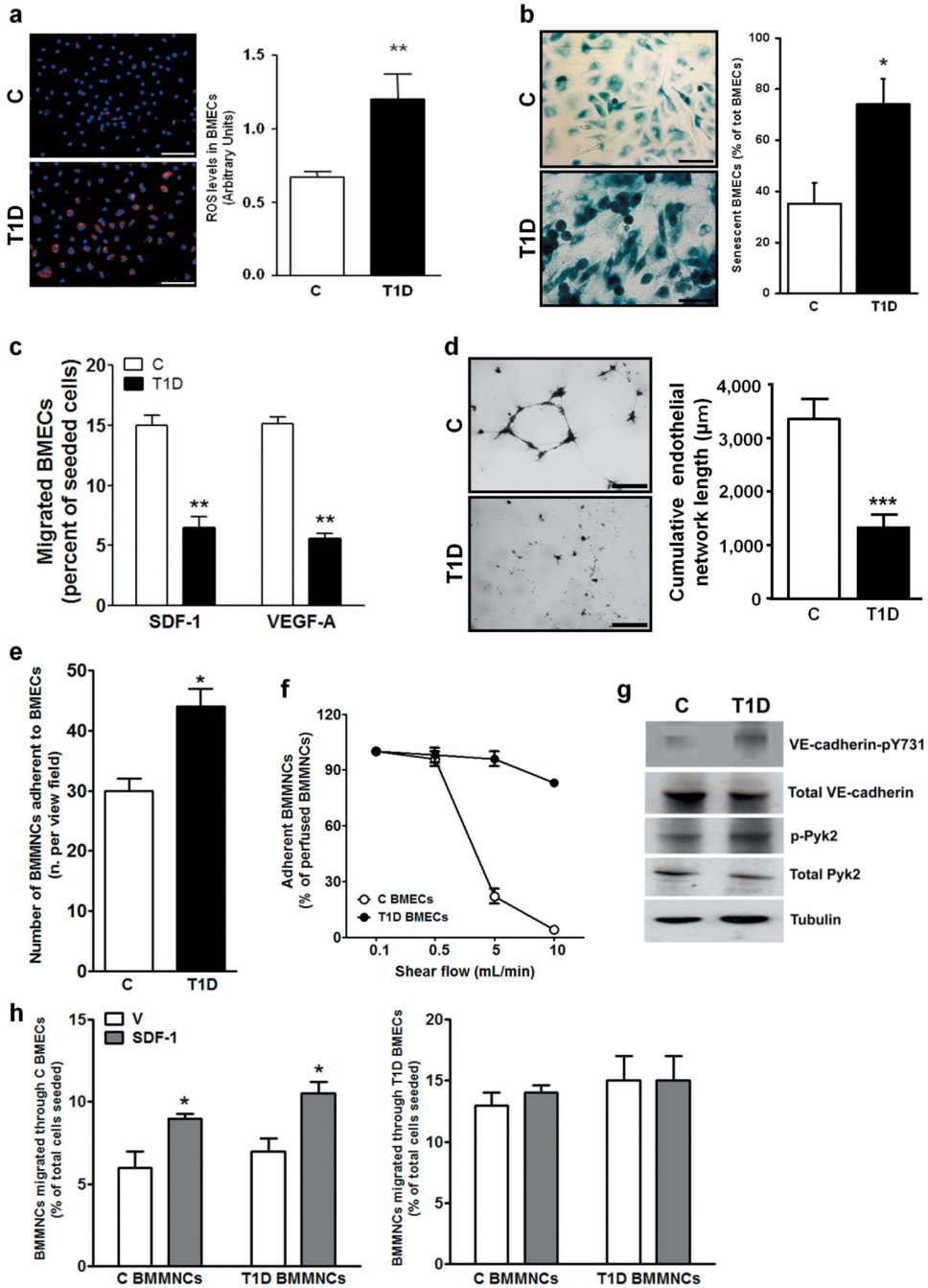


**Figure 3. T1D-induced phenotypic alterations of BMECs**

Microphotographs (scale bars: 100µm) and bar-graph illustrating ROS levels (a) and β-Gal activity (b) in BMECs. (c) Migration of BMECs toward SDF-1 and VEGF-A. (d) Endothelial network formation by BMECs plated on matrigel (Scale bars: 500µm). Adhesion of BMMNCs to non diabetic (C) BMECs or T1D BMECs under static conditions (e) and under the influence of shear flow (f). Western blot analysis of VE-cadherin-pY731 and Pyk2-pY402 (g). Trans-endothelial migration of BMMNCs towards SDF-1 (100 ng/mL) or vehicle (V) using BMECs isolated from C (h, left panel) or T1D mice (h, right panel)

seeded on transwell inserts. For each assay, three separate experiments in triplicates were averaged. \* $P < 0.05$ , \*\* $P < 0.01$  and \*\*\* $P < 0.001$  vs. C.

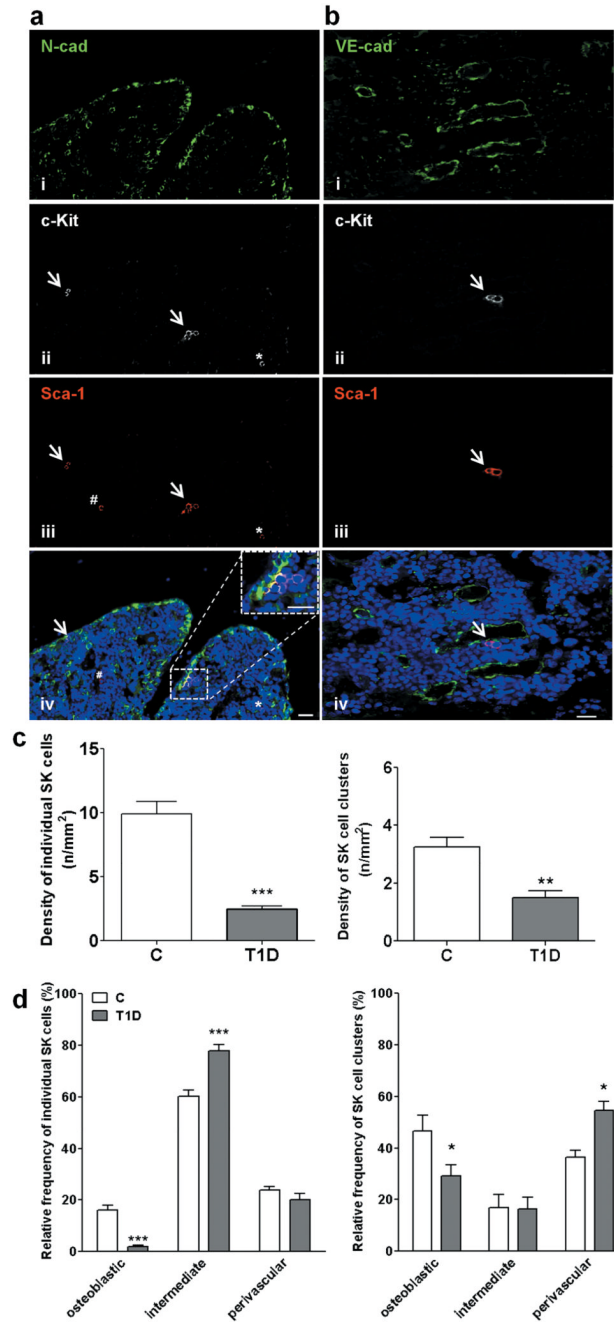


#### Figure 4. T1D reduces the abundance of SK cells

Microphotographs (a,b) and graphs (c,d) showing SK cells of the osteoblastic (N-cad) and vascular niche (VE-cad). An individual cell (\*) and clusters of cells (arrows) expressing c-Kit (ii) and Sca-1 (iii). Double-positive cells (purple fluorescence, iv). One cell expresses Sca-1 only (#). Scale bars: 20  $\mu$ m. n=7 mice per group. \* $P$ <0.05, \*\* $P$ <0.01 and \*\*\* $P$ <0.001 vs. C.



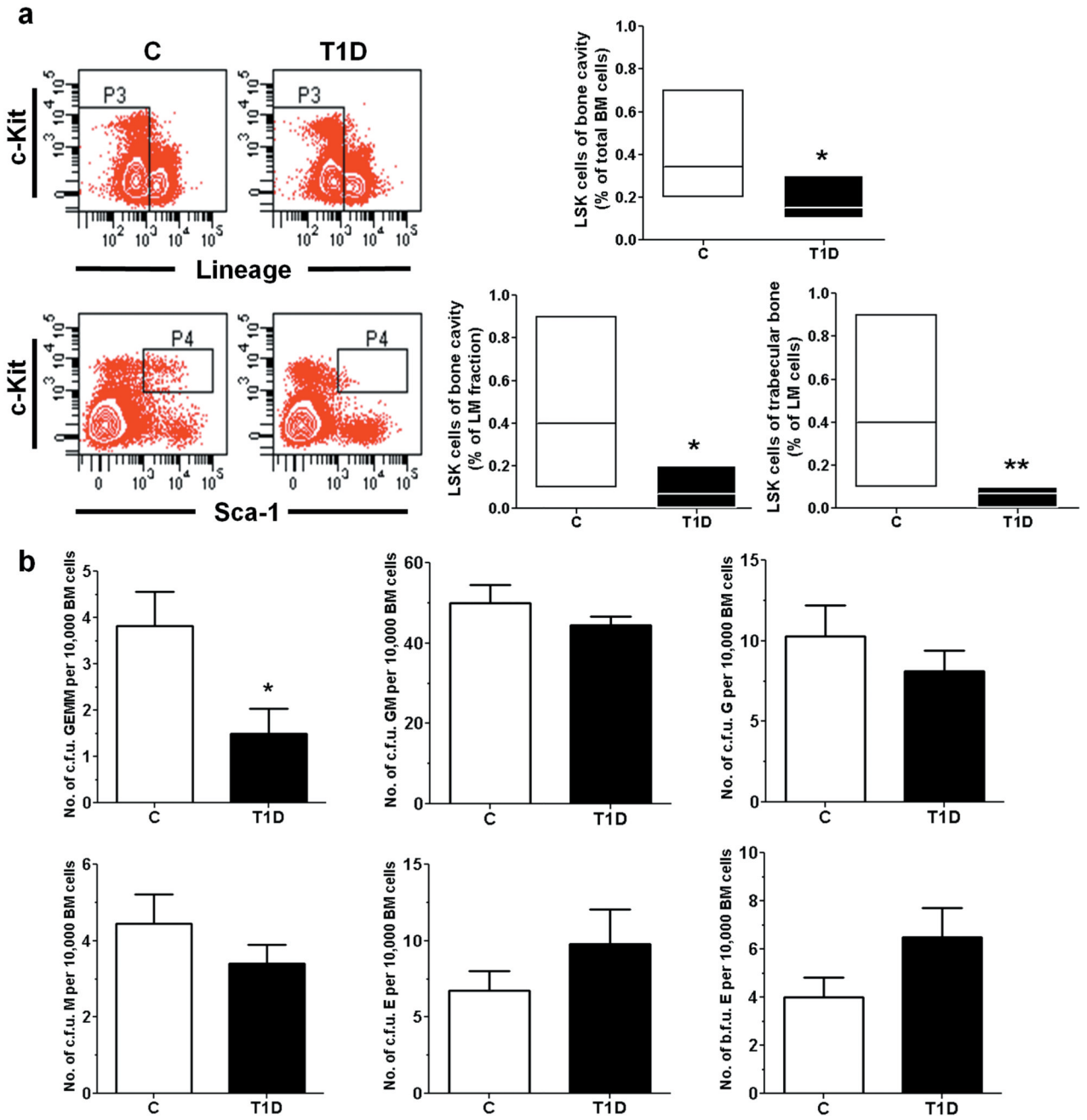


**Figure 5. T1D depletes BM LSK cells**

(a) Flow cytometry analysis of PI<sup>neg</sup> lineage<sup>neg</sup> c-Kit<sup>pos</sup> Sca-1<sup>pos</sup> cells. n=7 mice per group.

(b) Colony forming unit (c.f.u.) assay of marrow cells harvested from trabecular bone. n=5 mice per group. \*P<0.05, \*\*P<0.01 vs. C.

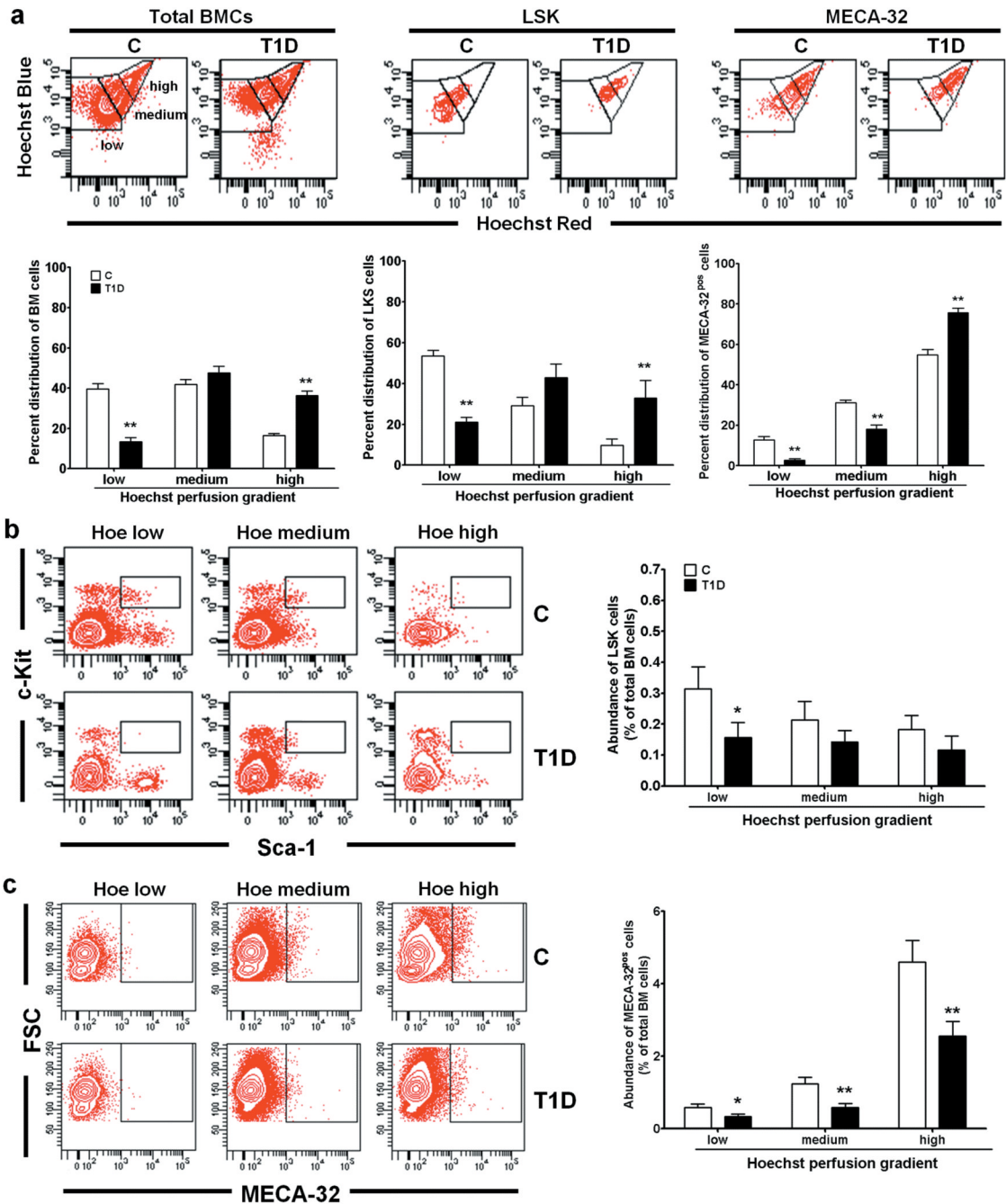


**Figure 6. Depletion of LSK cells follows perfusion gradient in diabetic BM**

(a) Representative plots of Hoe uptake by BM cells and percent distribution of cells across the perfusion gradient. Abundance of LSK cells (b) and MECA32<sup>pos</sup> ECs (c) in each level of perfusion gradient. n=7 mice per group. \* $P<0.05$ , \*\* $P<0.01$  vs. C.

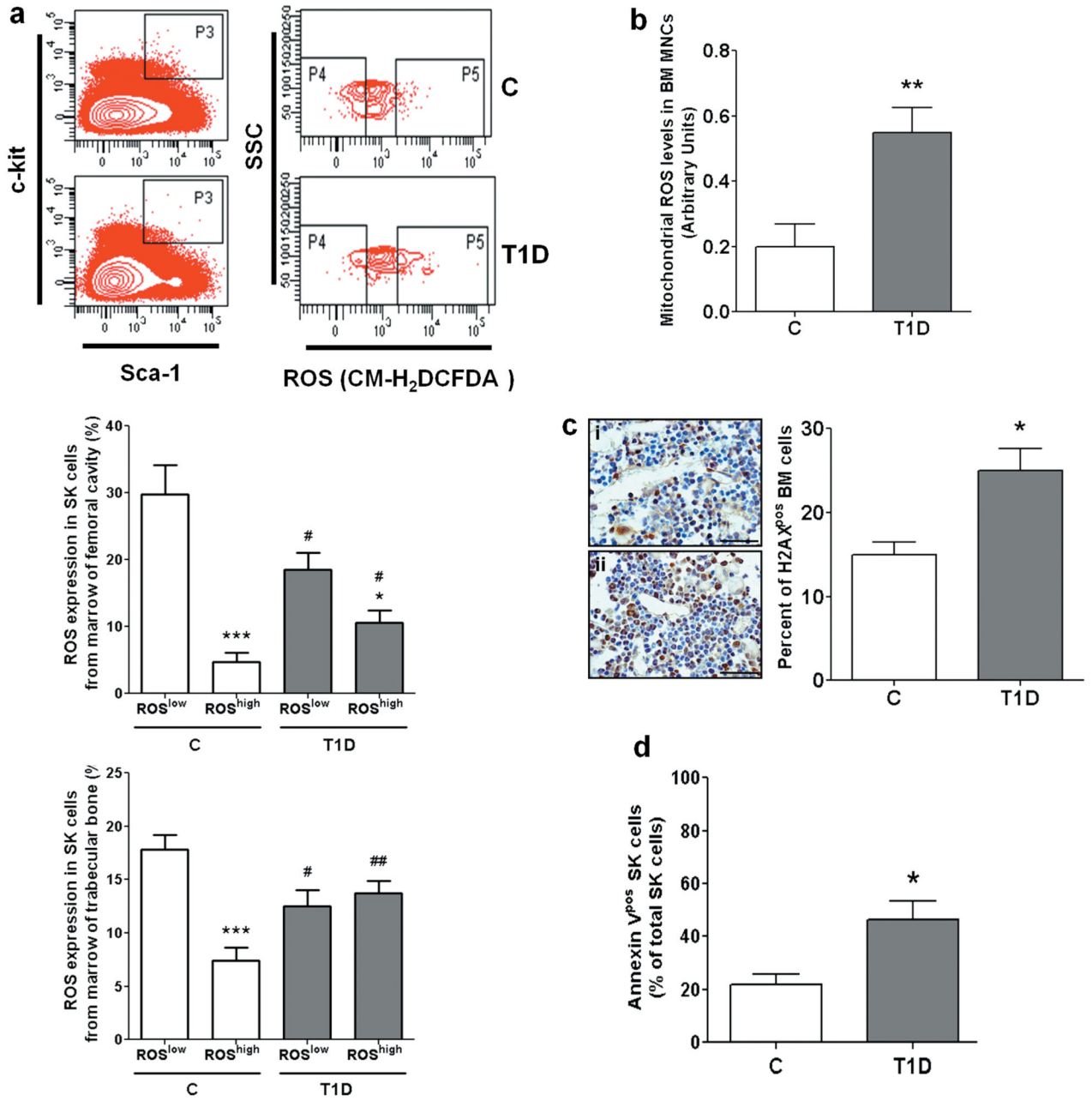


**Figure 7. Diabetes activates oxidative stress**

(a) Intracellular ROS assessed by CM-H<sub>2</sub>DCFDA; \**P*<0.05, \*\*\**P*<0.001 vs. ROS<sup>low</sup>, #*P*<0.05, ##*P*<0.01 vs. C (b) Mitochondrial ROS assessed by MitoTracker Red CM-H2XRos. (c) Levels of p-H2AX (*i*: controls; *ii*: T1D. Scale bars=50μm). (d) Annexin V<sup>pos</sup> SK cells. n=7 mice per group. \**P*<0.05, \*\**P*<0.01 and \*\*\**P*<0.001 vs. C.

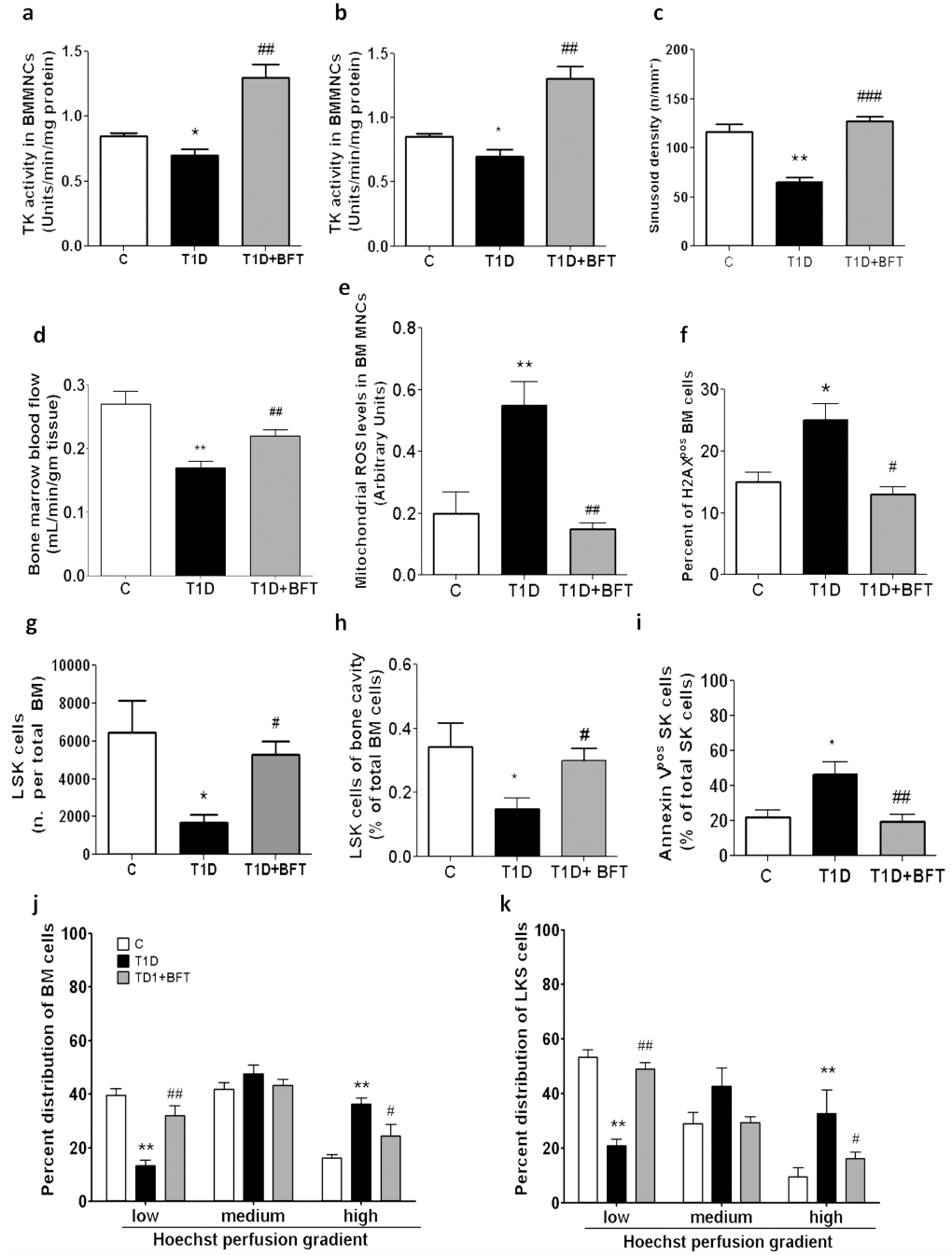


**Figure 8. BFT prevents microangiopathy**

Effect of BFT on transketolase (a) and G6PDH activity (b), sinusoid density (c), blood flow (d), ROS (e), and p-H2AX in BMMNCs (f). BFT prevents diabetes-induced depletion of LSK cells, assessed as absolute number (g) or percent of total BM cells (h), and reduces apoptosis (i). Bar graphs represent the percent of LSK cells in total BM cells (j) or LM (k) across the Hoe perfusion gradient. n=7 mice per group. \**P*<0.05, \*\**P*<0.01, \*\*\**P*<0.001 vs. C; #*P*<0.05 ##*P*<0.01, ###*P*<0.001 vs. vehicle.